Ionic debris measurement of three extreme ultraviolet sources

J. Sporre,[1] C. H. Castaño,[2] R. Raju,[1] and D. N. Ruzic[1,a)]
[1]*Department of Nuclear Plasma and Radiological Engineering, Center for Plasma Material Interactions, University of Illinois at Urbana-Champaign, 216 Talbot Laboratory, MC-234, 104 South Wright Street, Urbana, Illinois 61801, USA*
[2]*Department of Nuclear Engineering, Missouri University of Science and Technology, 222 Fulton Hall, 301 West 10th Street, Rolla, Missouri 65409, USA*

(Received 18 March 2009; accepted 15 June 2009; published online 19 August 2009)

Generation of debris in extreme ultraviolet (EUV) light sources is an inherent and real threat to the lifetime of collection optics. Debris measurement of these sources is useful to enable source suppliers to estimate collector lifetime. At the Center for Plasma Material Interactions (CPMI) at the University of Illinois, an Illinois calibrated spherical sector electrostatic energy analyzer (ICE) was built to measure the ion debris flux in absolute units. In addition to ion flux, the detector is also capable of identifying different ion species present in the plasma utilizing energy-to-charge ratio discrimination. The lifetime of the collector optics is calculated using the measured ion flux. In the current investigation we compare the measurement of ion debris production in three different EUV sources: the Energetiq EQ-10M, the AIXUV-100, and the XTREME XTS 13-35. In the EQ-10M source, three angular measurements are coupled with three variations in operating pressure to measure consequent effects on debris production. These measurements reveal four predominant ion species in the energetic debris analysis: C^+, Si^+, Xe^+, and Xe^{2+}. The amount of debris is reduced as pressure is increased. Various debris mitigation methods are implemented in the AIXUV-100 source and results reveal that four ion species are observed (Ar^+, Xe^+, Xe^{2+}, and W^+), though there does not seem to be a dominant species. The first mitigation technique, backstreaming argon toward the source, reduces the amount of Ar^+, Xe^{2+}, and W^+, yet increases the amount of Xe^+ The increase in Xe^+ flux is explained based on charge exchange phenomena. The ICE machine was then attached 1.92 m away from the pinch of XTS 13-35 source, and placed at 25° away from the normal line. The comparison of results reveals that the XTS 13-35 and the EQ-10M sources produced comparable amounts of energetic ion flux per watt of EUV light produced. The AIXUV-100 source generated more ion debris flux per watt of EUV light than the other two sources, though it should be noted that the AIXUV-100 source was capable of producing more than ten times the amount of EUV light power compared to any of the other sources. © *2009 American Institute of Physics*.
[DOI: 10.1063/1.3176494]

I. INTRODUCTION

The use of extreme ultraviolet (EUV) light as a future lithographic technology requires several obstacles to be overcome.[1] EUV light's high absorption into almost every substance prevents the use of a simple clear protecting barrier between the source and the collection optics, such as a window or some sort of spectral purity filter. Lacking such a barrier, all energetic debris created by the plasma sources used to make EUV light is able to collide with these mirrors. These collisions cause the degradation of mirror reflectivity due to erosion and contamination. Such a loss in mirror reflectivity decreases the mirror's lifetime and consequently increases the cost of ownership, which limits EUV lithography (EUVL) as a viable technology for the future.[2] Source manufacturers have various methods for reducing the expulsion of this energetic debris, but usually at the expense of the power of EUV light produced. With this tradeoff in mind, the Center for Plasma Material Interactions (CPMI) at the University of Illinois, in coordination with SEMATECH,[3] constructed a traveling Illinois calibrated spherical sector electrostatic energy analyzer (ICE) machine capable of measuring energetic ion debris flux. This device, which is capable of quantifying and characterizing the destructive debris produced by EUV sources, was sent to various source suppliers to measure their sources under different conditions in order to assist in detailing the tradeoff between debris produced and EUV power created. In this report, the following three sources are examined: the Energetiq EQ-10M,[4] the AIXUV-100,[5] as well as XTREME Technologie's Xe-Fueled XTS 13-35.[6] For each of these sources the total ion debris measured at each operating condition was compared to the amount of EUV light produced under similar conditions in order to produce a measurement of comparable relevance between each of the sources.

II. EXPERIMENT

A. Traveling ICE machine

The ICE machine utilizes a time of flight analysis system to measure ions of different energies. A Comstock[7] AC-902b spherical sector energy analyzer (ESA) with dual microchan-

a)Author to whom correspondence should be addressed. Electronic mail: druzic@illinois.edu.

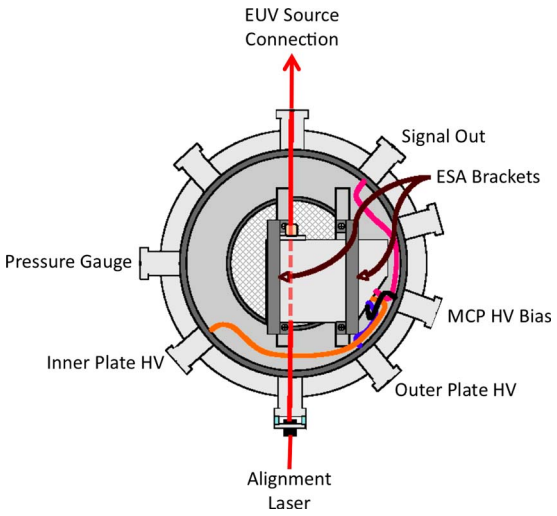

FIG. 1. (Color online) Schematic of the ICE and the corresponding component inputs.

nel plate (MCP) detectors from Burle[8] allows for a user to isolate ions based on their energy to charge ratio (E/q); ions with smaller ratios are deflected into the inner spherical sector, while ions with larger ratios pass into the outer spherical sector. The ions of interest are deflected into the first set of MCPs, creating an electron cascade, which is further amplified by a second MCP. This electron cascade produces a signal, which is modified using an Ortec 9326 fast preamplifier. The resulting signal ($\sim$150 mV–7 ns) is monitored using the histogram function on a 1 GHz Agilent[9] Infiniium DSO 8106a oscilloscope. The E/q isolation is established using two Spellman SLP300 HV power supplies to hold the inner and outer deflecting plates at opposite potentials, while a third Spellman power supply maintains a -2150 V bias across the two MCPs. The deflecting power supplies are capable of isolating up to 14 keV ions. A laser, attached at the rear of the ICE machine, allows for line of sight alignment of the ESA to the EUV plasma source (Fig. 1). Lastly, a Varian V550 Turbo pump in conjunction with a Varian SD-450 foreline pump evacuates the ICE chamber to the low 10^{-6} Torr by utilizing a 3 mm differential pumping orifice between the EUV source chamber and the ESA chamber. An 80/20 (Ref. 10) support apparatus is used to adjust the height of the ESA to accommodate the varying dimensions of sources.

B. Calibration

In order to extrapolate meaningful data from the ion signals generated using the MCPs, it is necessary to measure the sum all of the signals over a period of time using the histogram function on the oscilloscope. A 2 min data trial reveals a tally of the total number of hits occurring at a certain time period after the EUV plasma is created. Utilizing Eq. (1), which equates ion energy to kinetic energy, it is possible to use the known distance from the plasma source (L) to correlate the measured delay to a given ion energy.

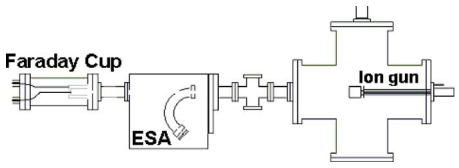

FIG. 2. (Color online) Schematic of the ESA calibration system. The ESA is calibrated by measuring the current created using an ion gun, and comparing it to an ion measurement with the ESA.

$$qE = \frac{1}{2}m\left(\frac{L}{t}\right)^2. \tag{1}$$

From this knowledge, a total number of "hits" are attributed to a certain ion species/charge state. It is necessary to calibrate the ESA for different measured ion energies in order to turn the number of hits measured into a quantifiable number of ions. Such a calibration is accomplished utilizing an IQE 11/35™ ion gun in coordination with a Faraday cup to create a calibrated ion to hit ratio as shown in Eq. (2).[11] The calibration setup is shown in Fig. 2.

$$N_i(E) = \frac{X(E)\frac{I}{e}tP}{X(E=1\ \text{keV})\frac{\xi(E)}{\xi(E=1\ \text{keV})}}. \tag{2}$$

In Eq. (2), $N_i(E)$ is the number of ions at a given energy E, $X(E)$ is the measured number of hits at a given energy E (taken from the histogram), I is the current measured from the Faraday cup during calibration, e is the elementary charge (1.6×10^{-19} C), t is the measurement time during calibration, P is the percentage of ions contributing to the observed current that have energy E, and $\xi(E)/\xi(1\ \text{keV})$ is the detector efficiency at the given energy divided by the detector efficiency at 1 keV both from manufacturer data.

C. Measurement of the Energetiq EQ-10M source

The EQ-10M source is a discharge-produced plasma (DPP) EUV light emitting device. The particular machine measured for this experiment was located at the University of Albany in New York. Given space constraints, the ICE machine was installed at a distance of 2.25 m away from the pinch plasma. A secondary turbo pump was installed onto the drift tube, between the source and the tool, as a means to reduce the effect of stagnant neutral gas on reducing the number of ions reaching the tool. In the experiment, three angular measurements were coupled with three variations in operating pressure to measure consequent effects on debris production. The resulting debris measurements at each condition were then compared with the 11 W ($\pm1\%$ bandwidth) of EUV light in a 2π solid angle, in order to determine a resulting ion flux per watt of EUV light. It should be noted that this source was measured without any additional debris mitigation techniques, as were performed with the other two measurements.

TABLE I. The various experimental debris mitigation techniques used in the AIXUV-100 source.

Expt.	Debris mitigation technique
1	Without Ar backstreaming
2	With Ar backstreaming
3	Magnetic beamline with Xe backstreaming
4	Magnetic beamline with Ar and Xe backstreaming
5	Foil trap and Xe backstreaming
6	Foil trap with Ar and Xe backstreaming

D. Measurement of AIXUV-100 source

The second debris analysis was performed on the AIXUV-100–10 kV (2001 version) source located at the AIXUV facility in Aachen, Germany. The setup of the experiment consisted of 1.11 m long drift tube between the source and the ICE machine. Two 5 mm orifices segmented the drift tube; the subsequent stagnant volume was pumped on with an additional turbo pump. In total, six experiments were performed on this machine, each of which involved the addition of various debris mitigation methods as described in Table I.

The addition of Ar and Xe backstreaming was introduced on the source side of the first 5mm orifice and simply consisted of flowing gas toward the pinch. The magnetic beamline experiments consisted of adding a set of strong permanent magnets placed in a manner to deflect ions and electrons in such as way that they do not propagate very far away from the source chamber. The last debris mitigation method consisted of installing a newly developed foil trap between the source and the ICE machine.

E. Measurement of XTREME Technologies XTS 13-35 source

The last source measured was the XTS 13-35 source, which was located at the University of Illinois at Urbana-Champaign.[12] This source was used as a reference measurement in order to provide a comparison between the two previously unmeasured sources and the well-documented debris characterization of the XTS 13-35. In this regard this measurement acted as a step toward standardization. The XTREME Commercial EUV emission diagnostic system consisted of the source and an attached test chamber, which provided various access points for analyzing the EUV plasma. There were two primary methods of debris mitigation in place within the chamber: a collimating foil trap, and the use of an argon buffer gas. The buffer gas was introduced in a showerheadlike manner near the pinch and provided a curtain of stagnant gas between the source and the foil trap. This particular experiment was performed using 200 (SCCM) (SCCM denotes standard cubic centimeters per minute at STP) of Ar flow. An Osaka Magnetically levitated TG-2300M pump maintained an operating pressure of ~3 mTorr at the chamber wall. The ICE machine was attached 1.92 m away from the pinch, and was placed at 25° away from the normal line. There are only a select few angles which provide direct line of sight to the pinch given that the debris tool contains a cooling component which block anything less than 20°. This particular experiment was performed without any Ar buffer gas, though previously published results reveal the effect Ar buffer gas has on debris mitigation in the XTS 13-35.[11]

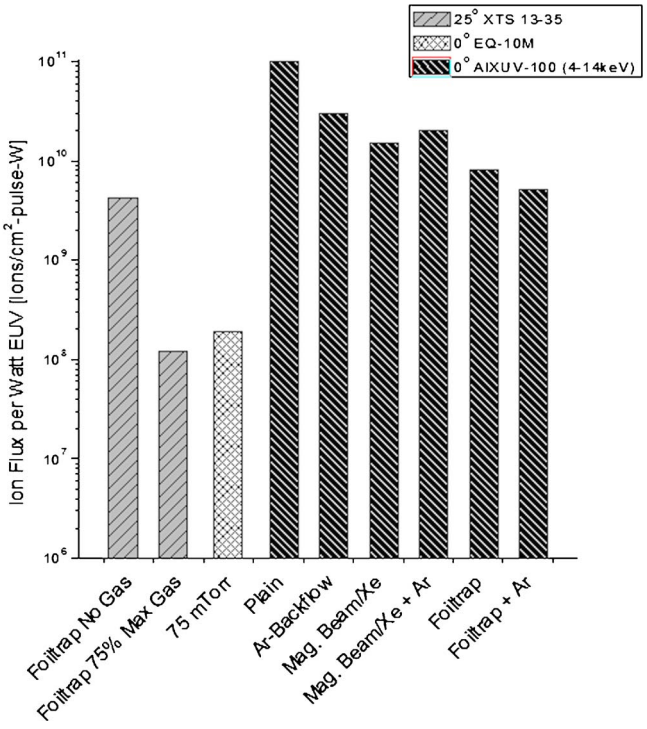

FIG. 3. (Color online) A comparison of ions debris flux per watt for all three sources EQ-10M, AIXUV-100, and XTS 13-35, with distance normalized to 1.92m for comparison purposes.

III. RESULTS AND DISCUSSION

A. Determining relative fluxes

In order to compare each source, it was necessary to diminish the source dependent variables involved in each source. Evidently there were two such factors that were of concern: the power to debris ratio, as well as the distance away from the source each measurement was taken. The first of these concerns presents an issue because debris mitigation methods not only decrease debris, but also decrease the amount of EUV power that is transmittable to the intermediate focus. One of the goals of this experiment was to explore this tradeoff; the power comparison is included in Fig. 3 to show how flux measurements varied in terms of power as well. As was mentioned earlier, the EQ-10M, AIXUV-100, and the XTS 13-35 sources were measured at 2.25, 1.11, and 1.92 m, respectively. Since the resulting plots are described in terms of flux, there is clearly a need to accommodate the $1/r^2$ variation between these measurements. Because the XTS 13-35 source was the first measured source, in order to make the EQ-10M and AIXUV-100 flux values comparable, their ion flux values were multiplied by a factor of 1.33 and 3.24, respectively, in order to get flux values at a length of $L_{adj}=1.92$.

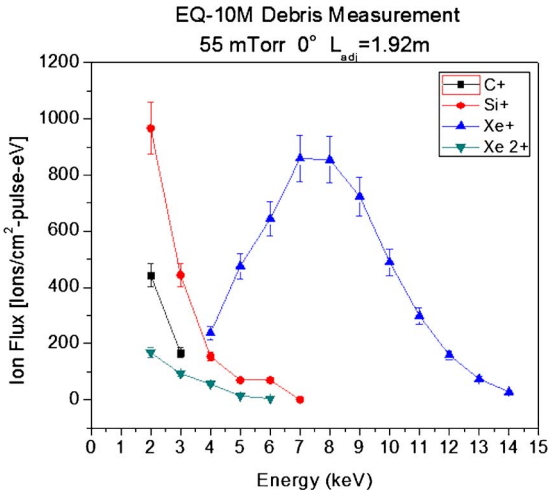

FIG. 4. (Color online) A full ion species analysis of the EQ-10M source at 0° and 55 mTorr. (L=2.25 m, L_{adj}=1.92 m).

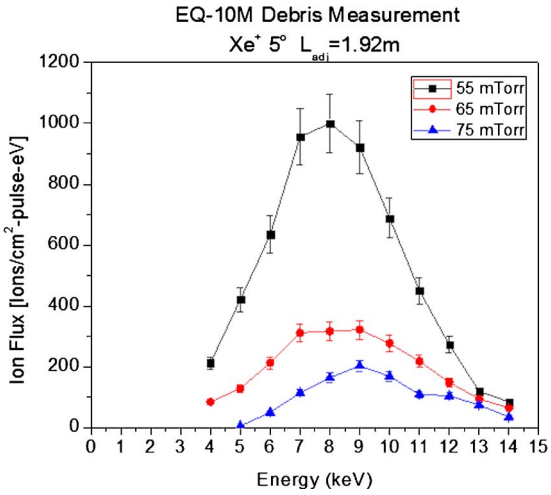

FIG. 6. (Color online) A plot of the effect of pressure on Xe^+ flux on the EQ-10M at 5° and K=4.5° shows a decrease in ion flux with an increase in pressure. (L=2.25 m, L_{adj}=1.92 m).

B. Energetiq EQ-10M debris analysis

The measurements of each of these sources provided some insight into the effects of varying operating conditions on the resulting amount of debris produced. The first source measured, the EQ-10M, revealed four predominant ion species in the energetic debris analyzed: C^+, Si^+, Xe^+, and Xe^{2+}. As can be seen in Fig. 4, at energies above 4 keV the Xe^+ ions dominate all of the other species and as such the comparisons at different operating conditions are only plotted with regard to the Xe^+ species. Figures 5–7 show that clearly the amount of debris was drastically reduced as pressure was increased. This too was coupled with an increase in total EUV radiation power as noted by Energetiq, who provided the information regarding the EQ-10M's EUV light emission capabilities. More notable was the larger effect on lower pressures than higher pressures; the logarithmic scale of Fig. 8 more dramatically displays the apparent effect of pressure on lower energies. It was also evident that, with an increase in stagnant pressure, the maximum ion flux occurred at higher energies. This change in peak energy can be attributed to charge transfer occurring more readily at lower energies. The future addition of a neutral detector to the ICE machine would more assertively define this assumption as it would be noticeable to see an increase in total neutrals with this decrease in energetic ion debris.

Figures 9–11 diagram the changes in energetic debris caused by moving off of the centerline axis. While plotted in these graphs for comparison, the 5° port data was actually fabricated in some regards. In post experiment analysis it was realized that an alignment error must have occurred in the taking of that particular set of data; not only were the ion fluxes much lower than should be anticipated relative to the other two angles, but it was also noted that physical manipulation of the connecting apparatus was needed to make the 5° adapter fit properly. As such, a corrective multiplier was used to correlate the lower energy (4–7 keV) fluxes of the 5° data to those of the other two angles. This sort of fit was appropriate given that lower energies are mostly isotropic (as opposed to the higher energies, which anisotropically favor

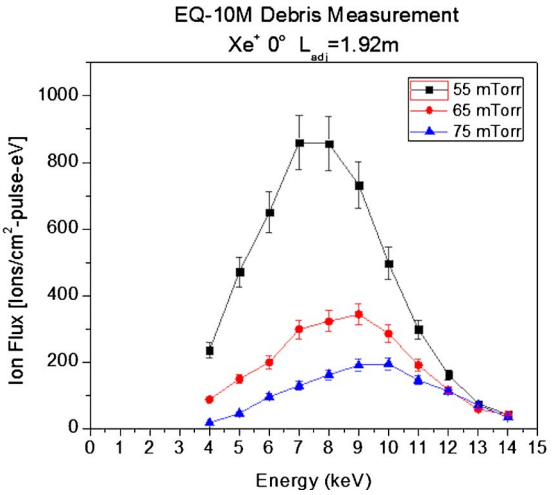

FIG. 5. (Color online) A plot of the effect of pressure on Xe^+ flux on the EQ-10M at 0° shows a decrease in ion flux with an increase in pressure. (L=2.25 m, L_{adj}=1.92 m).

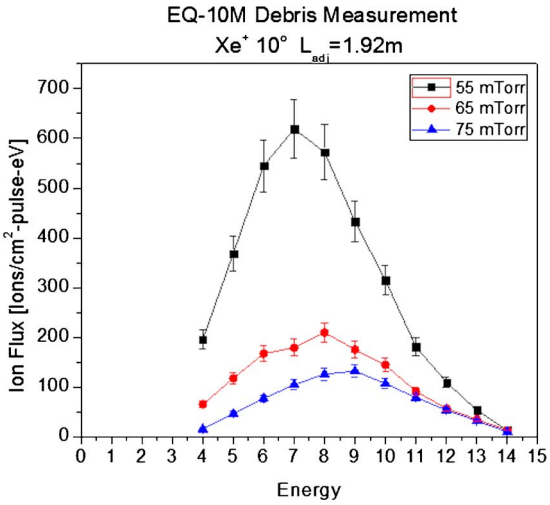

FIG. 7. (Color online) A plot of the effect of pressure on Xe^+ flux on the EQ-10M at 10° shows a decrease in ion flux with an increase in pressure. (L=2.25 m, L_{adj}=1.92 m).

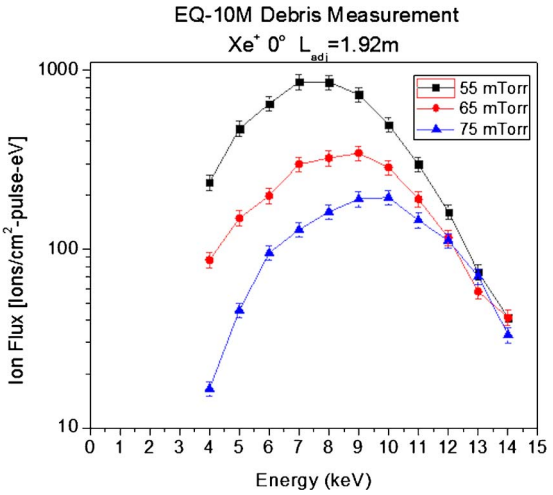

FIG. 8. (Color online) Effect of neutral pressure on high and low energy Xe^+ fluxes at 0° measurement (K=4.5, L=2.25 m, L_{adj}=1.92 m).

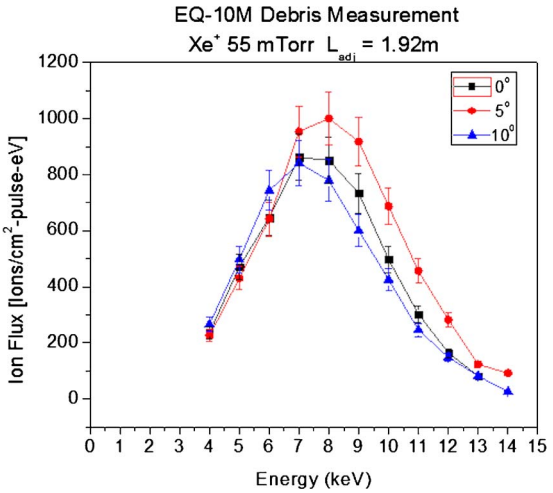

FIG. 9. (Color online) Angular measurement of Xe^+ flux on the EQ-10M for 55 mTorr and K=4.5 (L=2.25 m, L_{adj}=1.92 m).

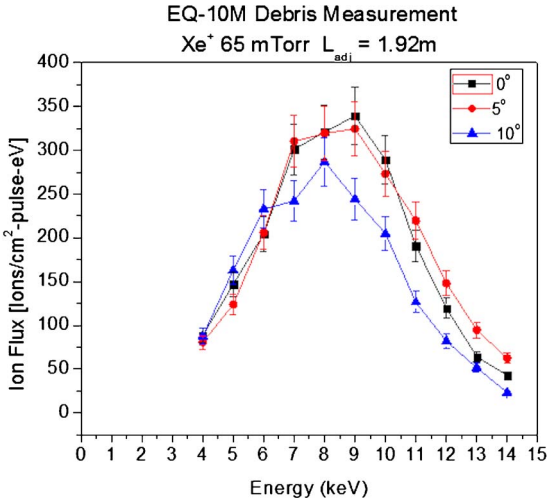

FIG. 10. (Color online) Angular measurement of Xe^+ flux on the EQ-10M for 65 mTorr and K=4.5 (L=2.25 m, L_{adj}=1.92 m).

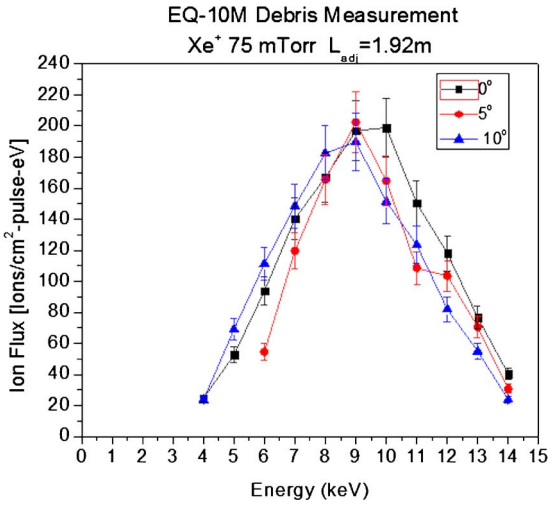

FIG. 11. (Color online) Angular measurement of Xe^+ flux on the EQ-10M for 75 mTorr and K=4.5 (L=2.25 m, L_{adj}=1.92 m).

lower angles), yet the presence of a corrective factor limits the ability to establish trends with this data. Examining the other two data sets, there is an evident trend showing the anisotropic nature of these higher energies.

C. AIXUV-100–10 keV (2001 version) debris analysis

The analysis of the AIXUV source revealed a much different ion behavior as seen in Figs. 12–15. Indeed out of the 4 remarkable ion species observed (Ar^+, Xe^+, Xe^{2+}, and W^+), there was not a single dominant species. In fact there was not a clearly observable maximum flux in any of these ion species. With regard to simple debris mitigation alone, the measurements revealed that the foil trap with argon backstreaming provided the best tradeoff between ion flux and EUV power. In terms of total power, a characteristic critical in EUVL, this tradeoff reduced the AIXUV-100 s power output by 90%. The method of backstreaming argon toward the source reduced the amount of Ar^+, Xe^{2+}, and W^+, yet increased the amount of Xe^+. The easiest explanation for such

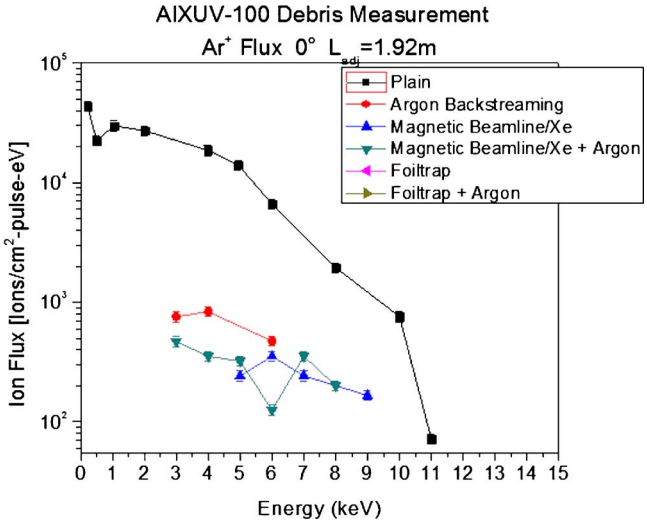

FIG. 12. (Color online) A comparison of Ar^+ flux for various methods of debris mitigation on the AIXUV-100 source. The error bars are present but drawn small due to the logarithmic nature. (L=1.11 m, L_{adj}=1.92 m).

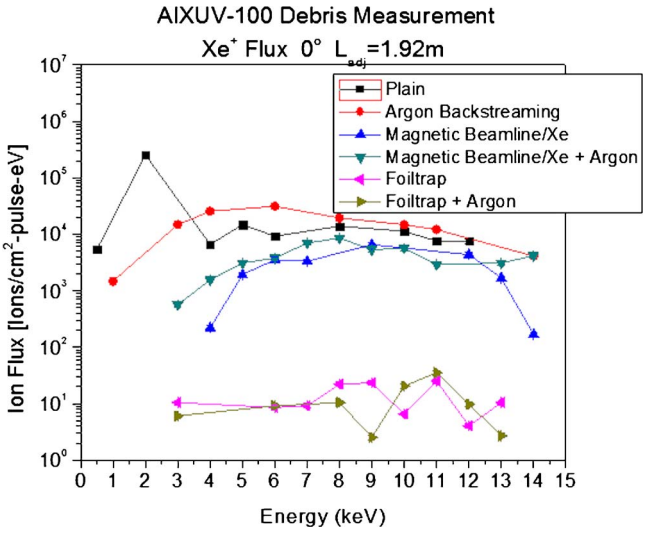

FIG. 13. (Color online) A comparison of Xe^+ flux for various methods of debris mitigation on the AIXUV-100 source. The error bars are present but drawn small due to the logarithmic nature. (L=1.11 m, L_{adj}=1.92 m).

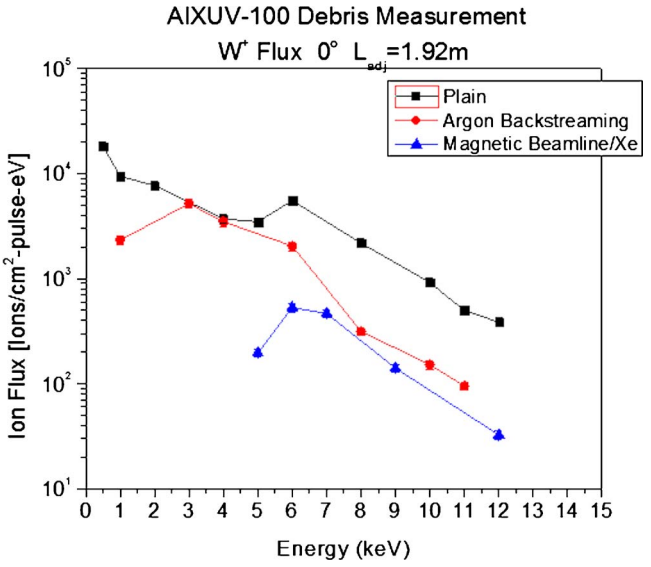

FIG. 15. (Color online) A comparison of W^+ flux for various methods of debris mitigation on the AIXUV-100 source. The error bars are present but drawn small due to the logarithmic nature. (L=1.11 m, L_{adj}=1.92 m).

an increase is the concept of charge exchanged mentioned earlier. While the method reduced the number of Xe^{2+} ions observed, it is likely that these ions simply picked up an electron and became Xe^+ ions, thus increasing the total flux of the singly ionized atom. The use of a magnetic beamline also behaved interestingly as well, attenuating higher energies by a factor of 4, while only reducing lower energy fluxes by a factor of 3. The magnetic beamline, created by placing magnets around the source to create a magnetic field around the source point, acts to confine charged particles using the Lorentz force. Retaining the high-energy ions allowed them to lower their energies through momentum exchange before they were ejected away from the pinch in a collision process. The increase in ion flux at all energies with the introduction of Ar backstreaming and the magnetic beamline suggests that there are more collisions allowing trapped ions to dislocate themselves from the magnetic field lines. Furthermore, as can be seen in Table II there is an increase in EUV absorption.

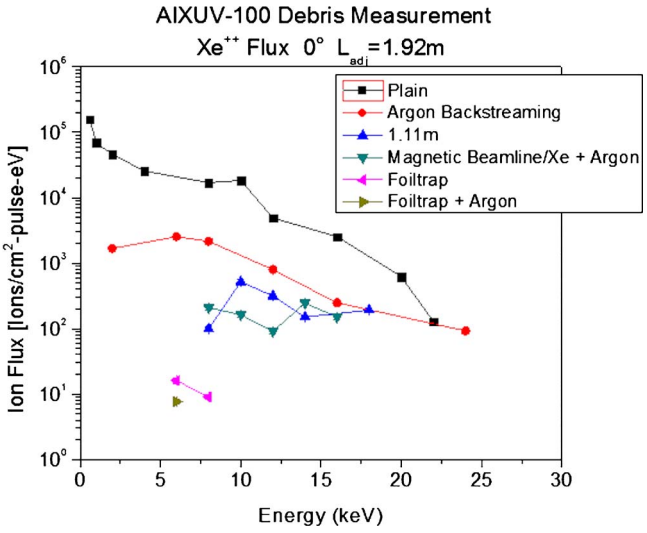

FIG. 14. (Color online) A comparison of Xe^{2+} flux for various methods of debris mitigation on the AIXUV-100 source. The error bars are present but drawn small due to the logarithmic nature. (L=1.11 m, L_{adj}=1.92 m).

D. XTREME Technologies XTS 13-35 debris analysis

The last source measured was the XTS 13-35. This system theoretically produced 35 W in 2π, yet measurements using a photodiode suggested that there was only a production of ~5 W. This reduction is most likely due to damage of the fins in the foil trap. As time progressed in operating the XTS 13-35, ion sputtering and collisions warped and displaced some of the fins nearest to the pinch, possibly causing a reduction in the throughput of light. The ion spectrum of Xe^+ was in stark contradiction to the predicted maximum energy of 8 keV for a DPP EUV source as shown in Fig. 16.[13] It was noted that in the lifetime of source operation the maximum flux progressively increased from ~8 keV to the 14^+ keV peaks where it was located at the time of the experiment. The four other predominant species were Xe^{2+}, Mo^+, W^+, and Ar^+. Xe^+ clearly made the other ion fluxes somewhat negligible, as there was a factor of 10 times the amount of debris. While power supply limitations prevented

TABLE II. Relative EUV light power outputs of various debris mitigation schemes for the AIXUV-100 source.

AIXUV-100 source configuration	EUV light emission (mW in 2π)
No debris mitigation	150[a]
Ar backstreaming	135
Magnetic beamline	111
Magnetic beamline with Ar backstreaming	100
Foil trap	16.6
Foil trap with Ar backstreaming	14.9

[a]The measurement without debris mitigation was known to AIXUV and the consequent debris mitigation EUV light power outputs were measured with a photodiode using relative calculations.

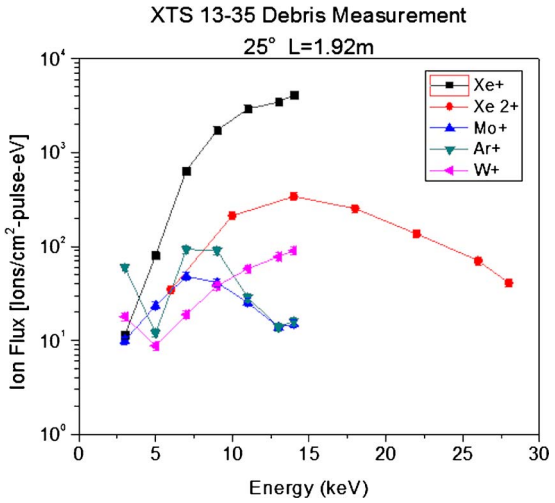

FIG. 16. (Color online) This figure shows the ion debris flux measured on the XTS 13-35 source at 25° offset from the centerline. There was no buffer gas present in this measurement. The error bars are present but drawn small due to the logarithmic nature. (L=1.92 m, L_{adj}=1.92 m).

measuring 1+ ions at energies higher than 14 keV, given the nature of the source in the past, it is appropriate to assume that the Xe^{+} flux peaks near 14 keV in similar fashion to the Xe^{2+} peak.

E. Comparison of sources

While each of the sources operated in completely different manners, with different end product goals in mine, it was possible to compare the sources based on the amount of debris produced per watt EUV produced. As can be seen in Fig. 3, the XTS 13-35 and the EQ-10M sources produce comparable amounts of energetic ion flux per watt. Moreover, although the AIXUV source produced more flux per watt than the other two sources, it should be noted that the AIXUV source was capable of producing more than 10 times the amount of EUV compared to any of the other projects.

IV. CONCLUSION

The EUV light lithography milestone, as established by the International Technology Roadmap for Semiconductors (ITRS)[14] is rapidly approaching. The ITRS is a collaborative effort within the industrial community to lay out a plan for the advancement of semiconductor technology in a cost effective manner. In order to achieve goals set by the ITRS roadmap, the high power sources must be capable of producing clean EUV photons. With this in mind it is necessary for source manufacturers to be able to measure the energetic debris produced by their machines. Not only will this determining measurement provide insight into the cleanliness of their machines, but it will also allow for source optimization and the extension of collector optic lifetimes. In this respect the XTS 13-35, the EQ-10M, and the AIXUV-100 were analyzed using the ICE machine developed at the Center for Plasma Material Interactions at the University of Illinois in conjunction with SEMATECH. It was found that the minimum amount of debris per watt EUV was provided by the XTS 13-35 source with approximately 1.2E8 ions/cm^2-pulse-W being produced; the EQ-10m produced roughly 1.5E8 ions/cm^2-pulse-W, and in its most effective method of debris mitigation, the AIXUV-100 ejected nearly 5.2E9 ions/cm^2-pulse-W. While neither of these machines may represent the most recent technologies, they serve as a stepping-stone for benchmarking future advances in EUV source technology.

ACKNOWLEDGMENTS

Without the help of many people, the traveling ESA would not be possible. At the University of Albany, where the Energetiq source was characterized, we received a great deal of assistance from Professor Greg Denbeaux, Chimaobi Mbanaso, Rashi Garg, and Leonid Yankulin. Energetiq also helped out considerably as a great deal of effort was placed into accommodating our time of flight requirements. At the second site, AIXUV, Dr. Rainer Lebert, Christian Wies, and Bernhard Jaegle proved to be invaluable as they slaved away adding and removing mitigation techniques. Lastly we would like to thank SEMATECH (Contract No. 401681) for funding this project and helping coordinate the visits. These people made our trips a great deal easier than they could have been, and their kindness was invaluable.

[1]V. Banine and R. Moors, J. Phys. D **37**, 3207 (2004).
[2]U. Stamm, J. Phys. D **37**, 3244 (2004).
[3]C. H. Castano, D. N. Ruzic, S. N. Srivastava, K. C. Thompson, and J. Sporre, Proc. SPIE **6921**, 692137 (2008).
[4]ENERGETIQ, Inc., Woburn, MA, http://www.energetiq.com/html/euv.html.
[5]AIXUV GmbH, Aachen, Germany, http://www.aixuv.de.
[6]XTREME Technologies GmbH, Gottingen, Germany, http://www.xtremetec.de.
[7]Comstock, Inc., Oak Ridge, TN, http://www.comstockinc.com.
[8]Burle Electro Optics, Sturbridge, MA, http://www.burle.com.
[9]Aglient Technologies, Inc., Palo Alto, CA, http://www.aglient.com.
[10]80/20, Inc., Warsaw, IN, http://www.80/20.net.
[11]E. L. Antonsen, K. C. Thompson, M. R. Hendricks, D. A. Alman, B. E. Jurczyk, and D. N. Ruzic, J. Appl. Phys. **99**, 063301 (2006).
[12]K. C. Thompson, E. L. Antonsen, M. R. Hendricks, B. E. Jurczyk, M. Williams, and D. N. Ruzic, Microelectron. Eng. **83**, 476 (2006).
[13]D. N. Ruzic, S. N. Srivastava, K. C. Thompson, J. Sporre, C. H. Castano, and R. Raju, Proceedings of the SPIE Advanced Lithography Conference, 2008 (unpublished), Vol. 72, p. 6921.
[14]*EUV Sources for Lithography*, edited by V. Bakshi (SPIE, Bellingham, WA, 2006).